AN AUTOMATED METHOD FOR CRATER COUNTING FROM DIGITAL TERRAIN MODEL USING ROTATIONAL PIXEL SWAPPING METHOD

Satoru Yamamoto[1], Tsuneo Matsunaga[1], Ryosuke Nakamura[2], Yasuhito Sekine[3], Naru Hirata[4], and Yasushi Yamaguchi[5]. [1]National Institute for Environmental Studies, Japan (yamachan@gfd-dennou.org), [2]National Institute of Advanced Industrial Science and Technology, Japan, [3]The University of Tokyo, Japan, [4]The University of Aizu, Japan, [5]Nagoya University, Japan.

INTRODUCTION

Various techniques for image-based crater detection/extraction have been developed based on the pattern matching filtering technique and Hough transform [e.g., 1-4]. However, previous methods are not suitable for use in the automated algorithm for the crater age determinations. Although several of image-based methods have been used for the automated detection of circular features, they do not provide sufficient accuracy for age determination from datasets containing a large number of craters with various sizes. In addition, they involve many complicated preprocessing steps to remove noncircular features and noise components such as mathematical morphology operators. An alternative approach for the automatic extraction of impact craters is to use the digital elevation model (DEM) or digital terrain model (DTM) [5-7]. Detection of impact craters from the DEM/DTM can help avoid problems inherent to visual detection methods such as the sensitivity of the results to the conditions of solar illumination. However, previous methods did not fully utilize the DEM/DTM data which provides 3-D information, because they first converted the DEM/DTM data to binary images prior to the application of crater detection methods.

Recently, we develop a fully automated algorithm [8] for the crater age determinations based on the Rotational Pixel Swapping (RPSW), which uses a multiplication operation between the original DTM/DEM data and the rotated data to detect impact craters [9,10]. This method uses the rotationally symmetric pattern of the slope gradients and slope azimuth of the crater wall to detect the crater shape. We call this method RPSD (RPSW for DEM/DTM) hereinafter. Although it has been demonstrated that the model ages determined by the RPSD for the lunar highlands and mare regions are consistent with those determined by manual counting [8], it is also important to examine how the RPSD could detect not only simple craters but also the complex circular structures such as overlapping, complex, and eroded circular structures. Here, we introduce how the RPSD method detects the complex circular structures and then discuss the detection ability of the chain craters (catena) using actual remote-sensing data.

ALGORITHM

We explain the RPSD algorithm using DTM data obtained by the Japanese lunar explorer SELENE/Kaguya mission [11]. Fig. 1(a) shows a relief image for an area on the lunar surface from the DTM data, that includes elevation data $Z(x,y)$ at a pixel (x,y). From the $Z(x,y)$ data, we calculate the map $G(x,y)$ of slope gradient θ and the map $A(x,y)$ of slope azimuth α. For $G(x,y)$ and $A(x,y)$, we produce rotated images $G_{i,j,\phi}(x,y)$ and $A_{i,j,\phi}(x,y)$ for rotation angle ϕ centered at (i,j). Using $G_{i,j,\phi}(x,y)$ and $A_{i,j,\phi}(x,y)$, we then define the mapping function $H_{i,j}(x,y)$ as

$$H_{i,j}(x,y) = \prod_{k=0}^{N} U_{i,j,\phi=k\cdot\Delta\phi}(x,y)\cdot V_{i,j,\phi=k\cdot\Delta\phi}(x,y) \quad (1)$$

$$U_{i,j,\phi}(x,y) = \begin{cases} 1 & (\theta_{\mathrm{L}} \le G_{i,j,\phi}(x,y) \le \theta_{\mathrm{U}}) \\ 0 & (G_{i,j,\phi}(x,y) < \theta_{\mathrm{L}} \vee G_{i,j,\phi}(x,y) > \theta_{\mathrm{U}}) \end{cases} \quad (2)$$

$$V_{i,j,\phi}(x,y) = \begin{cases} 1 & (|A(x,y) - A_{i,j,\phi}(x,y) - \phi| \le \omega) \\ 0 & (|A(x,y) - A_{i,j,\phi}(x,y) - \phi| > \omega) \end{cases} \quad (3)$$

where N is the total number of rotated images, $U_{i,j,\phi}(x,y)$ corresponds to a map of the pixels with θ ranging from θ_{L} to θ_{U} in $G_{i,j,\phi}(x,y)$, and $V_{i,j,\phi}(x,y)$ is the map of the pixels which satisfy the RS condition for the slope azimuth, where ω indicates the permissible angle range under RS for the slope azimuth. Fig. 1(b) shows $A(x,y)$, where we can see the same color variation at each crater: i.e., from purple, blue, green, to yellow in the counter-clockwise direction. This color variation seen at each crater indicates the rotationally symmetry (RS) in the slope azimuth, by which the RPSD identifies the circular structures.

Fig. 1(c) shows $H_{i,j}(x,y)$ when the center point (i,j) is located at 'A' in Fig. 1(a), where we assume $\omega = 30°$, $\Delta\phi = 60°$, and $N = 5$. We can see a broken ring-like structure which corresponds to the largest crater seen in Fig. 1(a). Fig. 1(d) shows $H_{i,j}(x,y)$ when (i,j) is located at 'B'. Although the crater at 'B' overlaps the crater at 'A', only the wall of the crater centered at 'B' is extracted, while the broken ring-like structure is erased. Thus, $H_{i,j}(x,y)$ only extracts the crater wall located at (or near) the center of rotation (i,j), while the other components are automatically removed.

Note that there is no noise-component in Figs. 1(c) and (d), although we do not explicitly include any noise

reduction steps. This is because the noise components are regarded as non-RS patterns in the calculation of H, and H values for the noise components are automatically reduced to zero [9]. Thus, this can easily extract individual circular structures even for overlapping, complex, and eroded circular features with noise components.

To search for the center of the RS pattern (hereinafter, CRSP) in a target image, we use the following rotational symmetry function:

$$R(i,j) = \sum_x \sum_y H_{i,j}(x,y). \quad (4)$$

If the center of rotation (i, j) is near the CRSP, R is large. In contrast, if the center of rotation is far from the CRSP, R is small. Thus, a relatively large R value indicates that the point is located near or on the CRSP. Following the RPSW procedure of [9], for the detection of multiple CRSPs, we select all points whose R values are larger than a threshold value. We then determine the crater rim for each CRSP. Using the DTM data, we obtain the elevation profile $P(n)$ along one radial direction from a CRSP, and then calculate the slope gradient profile $Q(n)$ along the radial direction. From $Q(n)$, we search for the point whose slope gradient largely changes to find the rim.

In this method, one crater can be detected by multiple CRSPs. In order to avoid duplicate detections, we examine the relation between the crater radius and the distance between the two CRSPs. If, within the crater radius of a CRSP, there are CRSPs whose crater radii have already been determined, we regard the CRSP as a duplicate, and remove it from the list of candidate CRSPs.

APPLICATION TO COMPLEX CIRCULAR SATRUCTURES

We apply the RPSD to the chain craters, which are called the Catena Davy, near the Davy crater on the Moon. Fig. 2(a) shows the DTM data for the Catena Davy, where we can see a line of craters as the chain craters. Fig. 2(b) shows the results of the crater detection by the RPSD with $N = 7$ and $\omega = 30°$, where the detected crater rims are shown as yellow circles. Most of the chain craters are detected well without false detections.

SUMMARY

We demonstrated that this method succeeds in the automatic detection of not only simple craters but also complex crater structures such as chain craters, imperfect, eroded, and overlapping craters. In addition, the RPSD can be applied directly to the DTM/DEM data without any preprocessing such as binarization, and/or noise reduction. Furthermore, according to [8], the calculation time by the RPSD is several hundred times faster than previous methods using DTM data. We will also apply this RPSD to other complex structures such as the secondary crater fields and eroded craters on the Earth.

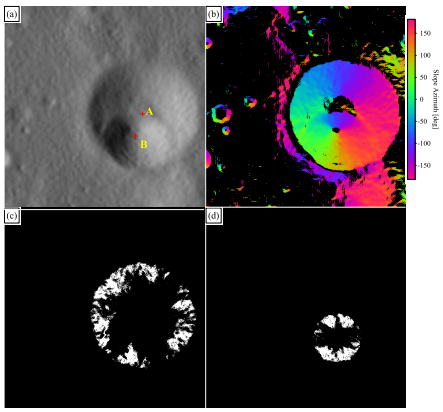

Figure 1: (a) Relief image from the DTM by TC [11]. (b) Mapping of slope azimuth for the surfaces with slope angles ranging from 10 to 33 deg from the surface. (c) Extracted image of $H(x, y)$ by RPSD for the center point at A in (a). The white indicates a value of 1 in $H(x, y)$. (d) The same as (c), but for point B.

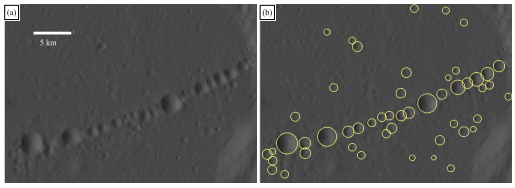

Figure 2: (a) DTM data for the catena (Catena Davy) on the Moon. (b) Result of crater detection by the RPSD method. Yellow circles indicate the crater rims determined by this method.

REFERENCES

[1] H. Taud & J.-F. Parrot, Int. J. Remote Sens., 13, 319, 1992. [2] M. C. Burl et al. Proc. i-SAIRAS, 6, 2001. [3] R. Honda et al., In Prog. in Discov. Sci., 2281, 2002. [4] Y. Sawabe et al., ASR, 37, 21, 2006. [5] B. D. Bue & T. F. Stepinski, IEEE TGRS, 45, 265, 2007. [6] G. Salamunićcar & S. Lončarić, IEEE TGRS, 48, 2317, 2010. [7] S. Lončarić et al., LPSC, 1454, 2011. [8] S. Yamamoto, S. et al., IEEE TGRS, 55, 4384, 2017. [9] S. Yamamoto, S. et al., IEEE TGRS, 53, 710, 2014. [10] J. Iisaka & T. Sakurai-Amano, Proc. Asian Conf. Remote Sens., OMPOO-13, 2000. [11] J. Haruyama et al., EPS, 60, 243, 2008.